Corrosion and Conservation of Lead in Sea Water

Ian Donald MacLeod,* Rhonda Wozniak
Department of Materials Conservation, Western Australian Museum, Cliff Street, Fremantle, Western Australia 6160

Abstract

Analysis of the corrosion products on lead artefacts recovered from historic shipwreck sites not only identifies the nature of the patina but it also provides an insight into the processes of decay across the site. From a comparison of the mineralogy of the lead corrosion products and their thermodynamic stability constants, it is possible to obtain a *corrosion map* of the areas from which the artefacts were recovered. This information provides the conservator and archaeologist with a new tool to gauge the effect of topography and water depth on the rates of deterioration of materials. The *corrosion maps* correlate with the levels of extractable chloride obtained from desalination data during treatment of artefacts. This data has general applicability regardless of the historical period pertaining to the wreck since lead is nearly always present on wreck sites. Corrosion simulation experiments in normal sea water provide an insight into the competing kinetic and thermodynamic forces that control the rate of deterioration of lead. The electrochemical data assists in the interpretation of the differences in patina.

Keywords

Corrosion, sea water, lead, desalination, electrochemical simulation, conservation

Introduction

A comparison of the corrosion products on lead and lead-alloy artefacts recovered from historic shipwrecks and the patinas of synthetic alloys exposed to oxygenated sea water indicated that the minerals might provide a good degradation indicator.[1] Corrosion products on pewters which had a lead content of 75 ± 10% showed a remarkable similarity to the minerals found on corroded lead artefacts from a similar environment.[1] The number of mineral phases identified as corrosion products from 99 ± 1% lead coupons, which had been corroded in natural seawater, was limited to four major and four minor corrosion products. Analysis of lead artefacts from a number of shipwreck sites produced a total of seven major and seven minor corrosion products. An initial analysis of the data on the distribution of the minerals amongst a dozen wreck sites indicated that the precise nature of the corrosion products depended on parameters that varied from site to site, more depending on the local environment than on the metal composition.

Despite the ubiquitous presence of lead artefacts in the form of sheathing, ballast pigs, musket balls, piping and scuppers on nearly all shipwreck sites, there is relatively little information on their decay problems in the conservation literature.[2,3] Since most of the artefacts are composed of 99 ± 1% lead there has been less of a priority to develop treatment procedures since the corroded artefacts are not normally subject to rapid decay in ambient storage. In the presence of volatile organic acids, such as acetic acid from wooden storage cabinets, the normally passive nature of these artefacts changes to one of aggressive decay.[4-7] Some new treatments have been developed to cope with these specific problems.[8]

In order to understand better the nature of the degradation processes that control the corrosion of lead in sea water, a number of experiments were performed to look at the effects of restricted oxygen access and simulated anaerobic bacterial activity, where sulphide ions were added to de-aerated sea water. Previous work has shown that electrochemical methods of studying the corrosion of historic metals can provide very useful information on why sections of the same object can corrode in a markedly different fashion.[9,10] The primary focus of the work has been on pure lead. A number of corrosion experiments were performed on synthetic and pure lead, to determine both the anodic behaviour and the nature of the corrosion products. These results were then compared with those found on artefacts from a number of shipwreck sites, in order to understand the correlation between the conditions of immersion and the nature of the corrosion process. The data was then checked against the information obtained from the treatment of real artefacts from a number of shipwreck sites. The influence of the alloying elements that are sometimes found in artefacts will also be discussed.

Corrosion simulation

The lead coupons were prepared from lead sheet that had a nominal purity of 99.9 wt % – details of the fabrication method for the 12 mm diameter cylindrical samples have previously been reported.[1] After being removed from the mould the samples were either sectioned and polished for metallographic analysis or converted into

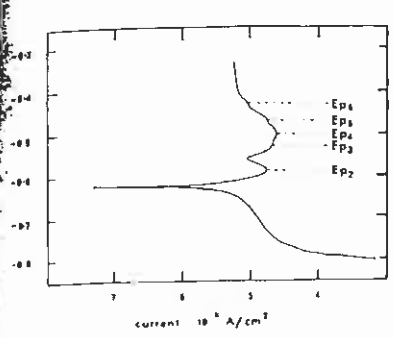

Figure 1 Plot of the log of the current density of a lead coupon, as a function of applied voltage, after four weeks of exposure to oxygenated sea water. The anodic peaks are noted as E_{p}

electrodes by soldering insulated copper wires to one face and then mounting the electrode in a polyester resin. The mounted samples were prepared by polishing with wet and dry carborundum papers to 1,200 grit and then with diamond to 1/4 micron. Microhardness measurements were made using a Tukon Model 300 microhardness machine using a 200 g load with a × 20 objective. The cast lead coupons were fairly uniform in physical properties with microhardness values (HV) of 7.1 ± 0.9 for longitudinal and 6.8 ± 0.8 for transverse sections.

Characterisation of the corrosion processes in aerated natural seawater on the coupons involved the use of ±250 mV scans at 0.5 mV s^{-1} from the rest potential. All the scans were performed in oxygenated sea water of 32‰ salinity. The voltage ramps and the subsequent log current voltage curves were generated by a Versastat EG&G Princeton Applied Research instrument. The reference electrode was a saturated calomel electrode and carbon rods were used as the auxiliary electrodes. Corrosion products on the artefacts and the pure lead electrodes were identified by X-ray diffraction. In order to understand the changing nature of the corroding lead surface, the cathodic and anodic potential scans were repeated, once the initial data had been collected, after intervals of 28, 60 and 70 days immersion in sea water. The results of the measurements, summarised in Table 1, show that the open circuit (corrosion) potential (E_{corr}) increases by 114 mV over 70 days and the corrosion rate, determined from the current voltage curves by the software, fell from 0.2 mm/year to 0.02 mm/year over the same time period. The lower corrosion rate equates to a 4 mm loss over 200 years – this is at the higher end of the observed range of metal loss. The corrosion potential, E_{corr}, is the mixed potential where the rate of oxygen reduction is equal and opposite to the rate of lead oxidation. The changes in corrosion potential and the corresponding drop in corrosion rates have been observed by other workers.[3] Plots of the log current–voltage curves showed the presence of up to five anodic peaks in any one scan, normally only three major peaks were observed in a single scan on an individual coupon. Where more peaks were found, the currents associated with the peaks indicated that they were minor components of the overall corrosion process. The current–voltage curve shown in Figure 1 is for lead after one month of exposure to oxygenated sea water. Control of corrosion will be related to passivation of local anodes and is strongly influenced by the reduction of dissolved oxygen and water. The data collected from all the scans is summarised in Table 1.

Although anodic peaks are normally associated with the formation of a specific corrosion products, only some of them could be clearly associated with the corresponding potential values. Surface analysis of the twelve corroded coupons, by scanning electron microscopy (SEM) and X-ray diffraction (XRD), shows that three major phases in each sample corresponded to three anodic peaks. The results of the mineral identification and peak location are included in Table 1. The presence of several major corrosion products on the surface of the lead coupons indicates that the oxidation of lead is associated with either sequential or simultaneous precipitation of corrosion products containing various proportions of chloride, sulphate, hydroxide and carbonate anions.[10,11] The complexes $PbCl^+$ and $PbSO_4$ are known to be labile whereas $PbCO_3$ and $PbOH^+$ are only partially labile in sea water.[11] Thus the availability of lead species at the corroding artefact surface is dependent on the surface pH since the overall activity of the chloride ions and carbonate ions will not change so readily. At pH 6–7 $PbCl_2$ is the dominant species and $PbCO_3$ predominates at pH 8–9 but the percentage of soluble lead as $PbCl^+$ is as high as 27% of all the dissolved species at pH 6. The passivated metal will still tend to dissolve.[12] The more porous nature of the structure of hydrocerussite ($Pb_3(CO_3)_2(OH)_2$) means that, where this mineral is the major corrosion product,

Table 1 Corrosion products and anodic peaks for pure lead coupons corroded in sea water at different immersion times (scan rate 0.5 mV s^{-1})

Sample history	Corrosion products by X-ray diffraction analysis	E_{corr} (mV vs SCE)	Peak potential (mV vs SCE)					
			E_{p1}	E_{p2}	E_{p3}	E_{p4}	E_{p5}	E_{p6}
Initial		−606				−497		
4 weeks	$PbCl_2$, PbCl(OH), $PbSO_4$, $Pb_3(CO_3)_2(OH)_2$, $PbCO_3$	−548		−587	−529	−497	−471	−436
10 weeks	$PbCl_2$, PbCl(OH), $PbSO_4$, $Pb_3(CO_3)_2(OH)_2$, $Pb_{10}(CO_3)_6O(OH)_6$	−527	−627	−587	−529		−471	
12 weeks	$PbCl_2$, PbCl(OH), $Pb_3(CO_3)_2(OH)_2$	−492	−627		−529			−436

the lead coupons or artefacts will corrode at a faster rate.[13] It is difficult unequivocally to assign all the anodic peaks to specific electrode processes since the corrosion of lead is controlled by the complex kinetics of the dissolution and precipitation reactions.

The results shown in Table 1 clearly show the difference between corrosion with a uniform access of the seawater to the lead surface and a localised restricted access which generates a more acidic condition and an increase in chloride activity. These variations in the corrosion conditions result in the formation of different compounds. An insight into the complexity of the reactions is seen by the extensive list of corrosion products found on the experimental coupons (Table 1) which had all been corroded in sea water but under somewhat different microenvironments.

The typical pH of lead coupons after seven months in a crevice corrosion cell was 6.57 and the chloride ion activity was 1.6 M,[1] or roughly three times the level associated with the standard exposure tests of four and ten weeks. The effect of the higher chloride content of the crevice cell is reflected in the greater proportion of chloride-containing lead corrosion products on the coupons. The greater acidity of the crevice solutions also is seen in a smaller proportion of hydroxy species than in the open-sea-water experiments. Details of the simple crevice cells, in which identical lead coupons were separated by 0.5 mm, can be found in reference 1. Despite the uncertainties associated with the values of the solubility products of the different mineral species, we are able to assign mineral phases to five of the six peaks. Because the experiments were performed on several coupons, the mineralogical analyses were performed on the replicate samples of the corroded surfaces which had not been scanned. In order to be identified by X-ray diffraction the corrosion products must be stable out of the experimental solutions. There was no correlation of the first peak at -0.627 (E_{p1}) with any of the available data; this may be a reflection of its inherent instability out of the low-voltage environment during the scan. The second anodic peak (E_{p2}) at -0.587 is probably due to formation of cerussite, $PbCO_3$, while E_{p3} at -0.529 is assigned to anglesite ($PbSO_4$). The fourth peak E_{p4} at -0.497 is due to the formation of $PbCl_2$; this is the only peak found in the initial scan of freshly polished lead in the oxygenated seawater. The fifth peak (E_{p5}) at -0.471 appears to be due to laurionite, PbClOH while the sixth peak at -0.436 is assigned to hydrocerussite, $Pb_3(CO_3)_2(OH)_2$.[14] It should be noted that the corrosion products identified in Table 1 are the total phases found on the sets of coupons exposed to the same environment and are not necessarily present on the surfaces of the coupons which gave rise to the anodic peaks.

On-site corrosion

The data base of *in situ* corrosion measurements on historic shipwrecks is dominated by information on iron and copper alloys, since these metals were the primary focus of the research activities. Thus on-site data on lead is limited to only two shipwreck sites.[1] Owing to the remoteness of the sites and the high cost of revisiting the wrecks, further data could not be obtained to support the work of this study. The corrosion potential of lead sheathing on the wrecks of the *Hadda* (1877) and the *Lively* (c.1820) was -0.473 ± 0.002 volts versus the saturated calomel electrode. These *in situ* corrosion potentials are at less negative potentials than any of the E_{p1} values measured on the coupons (Table 1) and are 233 mV more anodic than those found for freshly polished lead. The corrosion potentials correspond to the peak voltage associated with the formation of laurionite, PbOHCl. Both these shallow sites are characterised by well mixed oxygenated sea water. Since there is a characteristic voltage associated with the formation of mineral phases, the gradual shift in the corrosion potentials of the coupons will be associated with the formation of a variety of corrosion products. The presence of a mixed patina on the lead artefacts recovered from the *Hadda* and the *Lively* sites is totally consistent with the electrochemical data obtained from the coupons. Since the voltage of the anodic peaks is dependent on scan rate, all assignments remain tentative until the specific phases deposited on the surface at a specific voltage have been characterised. The important point to note is that the electrochemical methods of studying polarisation curves can provide a very sensitive indicator of the state of corrosion of the lead electrode materials.

Table 2. X-ray diffraction analysis of lead corrosion products on artefacts recovered from shipwreck sites

Name	Formula	*Zuytdorp*	*Vergulde Draeck*	*Batavia*	HMS *Sirius*	*Rapid*
Anglesite	$PbSO_4$	X	X	X	X	X
Cerussite	$PbCO_3$				X	X
Cotunnite	$PbCl_2$	X			X	
Galena	PbS					X
Hydrocerussite	$Pb_3(CO_3)_2(OH)_2$				X	X
Lanarkite	Pb_2OSO_4					X
Laurionite	Pb(OH)Cl				X	X
Litharge	PbO		X		X	
Mendipite	$Pb_3O_2Cl_2$		X			
Penfieldite	$Pb_2Cl_3(OH)$	X				
Phosgenite	$Pb_2(CO_3)Cl_2$				X	
Plumbonacrite	$Pb_{10}(CO_3)_6O(OH)_6$				X	

Apart from the activities of the constituent anions of hydroxide, chloride, sulphate and carbonate, the voltage associated with the corrosion of lead will depend on the solubility of the corrosion product. If the kinetics are rapid then the voltage will be determined by the thermodynamics of solubility product but if kinetic parameters, such as precipitation and hydrolysis reactions are significant, there will be a discrepancy between observation and theory. A comparison of the data in Table 1 and Table 2 shows that many of the mineral phases which have been identified on the surfaces of lead artefacts recovered after several centuries immersion in sea water are the same as in the test samples. The similarities of corrosion products are due to corrosion having occurred under similar physical conditions.

It is important for the discussion of these results that the nature of the wreck sites is noted. The *Zuytdorp* (1712) site is located at the foot of cliffs and is subjected to the full surge and turbulence of deep ocean waves breaking over the site. The wreck of the *Vergulde Draeck* (1656) is located amongst a series of gullies in a calcareous reef platform and is characterised by periods of intense wave action. The *Batavia* (1629) site lies inside a fringing coral reef and the *Lively* is distributed along a gully in a coral reef over similar depths to the *Batavia*. The wrecksite of the HMS *Sirius* is a dominated by a reef platform with water depths of 3.5–1.5 m at high tide. A series of gullies cross-sects the site, which is generally characterised by strong wave action. The most benign site is that of the *Rapid* which is in 7 m of water and protected from the full action of the waves by an offshore reef. Anglesite ($PbSO_4$) is a common corrosion product on all the sites. This mineral dominates the corrosion products on maritime lead artefacts. Observations on a wide number of artefacts where anglesite is the dominant corrosion product indicate that it is a passivating patina. Infrared spectral studies on rolled lead exposed in air for more than 100 years confirms that the lead sulphate patina is protective.[15] Some clear trends emerge when the distribution of the various corrosion products is correlated with the nature of the shipwreck sites. Minerals containing the oxide anions that were found amongst the corrosion products are associated with high-energy sites. The oxide sulphate lanarkite, the oxide chloride mendipite, the oxide hydroxy carbonate plumbonacrite and red lead oxide in the form of litharge were all found on high-energy sites.

There appear to be similarities across the range of sites where the corrosion products are largely influenced by the overall amount of water movement. Apart from the presence of the oxide and oxide/anion minerals already noted as being associated with turbulent waters, the *Zuytdorp* and the HMS *Sirius* show the presence of cotunnite ($PbCl_2$) as well as higher chloride containing minerals such as penfieldite, Pb_2Cl_3OH, on the *Zuytdorp* site. Since detailed site plans of the location of the particular lead artefacts are available for the *Sirius* it is possible to see what effects the differences in localised water movement have on the corrosion products. The oxide containing minerals litharge (PbO) and plumbonacrite ($Pb_{10}(CO_3)_6O(OH)_6$) were found only in the shallowest part of the site closest to shore where the waves constantly tumble (Figure 2). Calculations of the localised current flow on this site, during the descent of a typical 4 m wave breaking on the site at a water depth of 3 m, gives a resultant velocity of 12 m s^{-1} at an angle a little steeper than 45°.[17,18] The massive flux of dissolved oxygen across these areas means that the alternative reaction of hydrogen reduction is insignificant. The water movement will produce significant concentrations of hydroxide ions via reduction of oxygen.

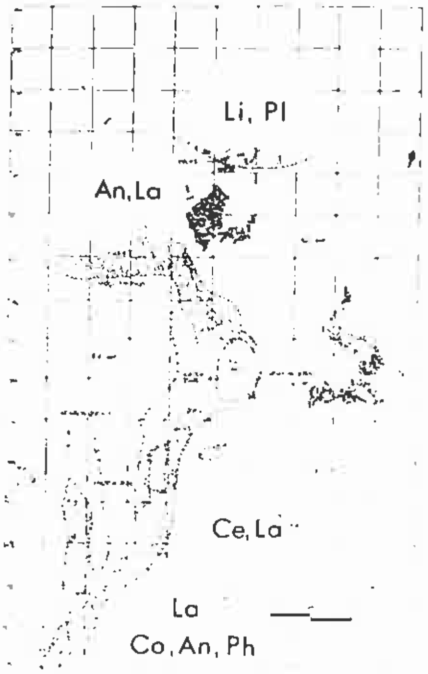

Figure 2. Site plan of the HMS Sirius wreck on Norfolk Island, showing distribution of lead artefacts and corrosion products. The mineral phases are Li(litharge), Pl(plumbonacrite), La(laurionite), An(anglesite), Ce(cerussite), Ph(phosgenite) and Co(cotunnite)

$$O_2 + 2H_2O + 4e^- \rightarrow 4OH^- \quad (1)$$

The localised increase in hydroxide ion activity will favour reactions such as

$$Pb + 2OH^- \rightarrow PbO + H_2O + 2e^- \quad (2)$$

over the formation of $PbCl_2$ or $PbSO_4$ as the major corrosion products. Studies on lead chloride electrodes confirm that the diffusion of oxygen to the artefact surface controls the formation of PbO.[19] The next set of lead artefacts on the *Sirius* site were found in a series of protected gullies in the reef platform, some twelve metres out to sea from the most turbulent part of the site, where litharge was a major corrosion product. In this area lead sulphate (anglesite, $PbSO_4$) was the dominant corrosion product, along with laurionite, PbOHCl. Anglesite was also the dominant mineral phase on most of the lead artefacts recovered from the sheltered waters of the *Rapid* site. A further 60 m from the worst of the surge, the corrosion products included the parent lead chloride cotunnite ($PbCl_2$) and the partly hydrolysed hydroxy-chloride, laurionite (PbOHCl), as well as the simple lead carbonate cerussite ($PbCO_3$) and smaller amounts of the basic carbonate hydrocerussite ($Pb_3(CO_3)_2(OH)_2$). Phosgenite ($Pb_2(CO_3)Cl_2$) was also found as a minor component on pieces of lead sheathing in this part of the site. The presence of so many mixed chloride–carbonates–hydroxycarbonates is a clear indication that there are a number of competing hydrolysis and precipitation reactions occurring during the corrosion of lead artefacts on the seabed. The presence of the double salts is consistent with the laboratory experiments which show that these corrosion products dominate the patina in still sea water.[13]

A schematic representation of some of the complex equilibria involving lead is as follows.

anglesite $PbSO_4$

↑

cerussite $PbCO_3$ ← cotunnite $PbCl_2$ → penfieldite Pb_2Cl_3OH → laurionite PbClOH

↓

hydrocerussite $Pb_3(CO_3)_2(OH)_2$

Although the normal pH of the sea water on the shipwreck sites was 8.15 ± 0.05 our crevice corrosion experiments indicate that significant differences in pH and chloride ion activity can readily develop under restricted access to flowing sea water. The lead sheet SI 66 had anglesite, laurionite and cotunnite as the major phases on the surface. If these species are in equilibrium, the calculated pH of the surface is 5.2 ± 0.2.[14-16] This pH may well occur in crevices, but since these minerals were found on the surface of the lead sheet it indicates that kinetic forces are dominant since the amount of water movement over all parts of the site is high at all times. Erosion phenomena from water-borne sand and grit will also be a major influence in determining which corrosion products ultimately survive on the surface of the artefact.

Dechloridation and conservation

Given the sensitivity of the lead corrosion products to act as an indicator of the corrosion energy of the different parts of a shipwreck site, it is important to the conservator to know the practical implications of this corrosion study. One practical consequence of the wide variety of corrosion products that form on the surface of lead artefacts is that the amount of chloride present in the corroded layers will vary significantly from site to site. These variations can also be significant across sites, as was illustrated in the case of the *Sirius*. The chloride content of the parent minerals falls from the highest value in $PbCl_2$ at 25.5 wt%, then penfieldite Pb_2Cl_3OH with 19.8 wt%, aurionite 13.65 wt% before and phosgenite $Pb_2CO_3Cl_2$ with 13.0 wt% laurionite PbClOH with 13.65 wt%. Quantitative surface analysis of a corroded lead ballast block from the *Zuytdorp* site had 19.3% chloride in the patina, which consisted of approximately 50% cotunnite, 25% penfieldite, 17% anglesite and 8% pseudoboleite ($Pb_5Cu_4Cl_{10}(OH)_8 \cdot 2H_2O$). A corroded lead sheet from the much calmer *Rapid* site had a patina of approximately 61% cerussite, 20% hydrocerussite and 19% laurionite, which gave the equivalent of 2.6% chloride in the

Table 3. Extracted chlorides (mg cm $^{-2}$) from desalination of lead artefacts

Zuytdorp(1712)	*Vergulde Draeck*(1656)	*Batavia*(1629)	*Lively*(c.1820)
High water flow	Aggressive reef	Deeper reef	Reef gully
3.7 (56)	64 ± 22	35 ± 20	25 ± 18

patina. Since most of the lead artefacts have been desalinated in bulk, there is limited data on the correlation between surface chloride content and bulk chloride deep within the corroded artefact. Since the lead artefacts range from massive 140 kg ballast pigs to 25 g musket balls, the normal comparison of extracted chlorides as a percentage of the artefact weight has little relevance, owing to the wide range of surface to mass ratios. One way to overcome this problem is to compare the amount of chloride extracted as a proportion of the corroded surface area. The results are summarised in Table 3.

The limited data set indicates that higher levels of chloride ions are associated with high-energy sites, but, as a result of flow velocity, the amount of chloride found in a patina does not always correlate with the overall nature of the site. The dozen *Zuytdorp* lead ballast pigs gave an average value of 3.7 mg cm $^{-2}$, which is consistent with the fact that only a few of the artefacts had been continuously exposed to the turbulent waters. The most corroded lead ballast pig gave a chloride extraction equivalent of 56 mg cm $^{-2}$. The site is also subject to significant changes in the sand levels in the area from which the lead ballast was recovered.[20] Because lead rapidly reaches a passivation state, the corrosion rates tend to average out over centuries. Our data listed in both Tables 1 and 2 clearly show that the nature of the patina on lead artefacts involves a very complex series of precipitation and dissolution reactions. Assuming a very crude linear law can be applied, the desalination of lead musket balls from a wide number of sites showed that the mean value is 0.028 ± 0.013 mg cm $^{-2}$ yr $^{-1}$. These data provide a guide to the conservator who is treating this type of material for the first time, by allowing an estimate of how much chloride is to be expected to be removed during desalination.

Effects of impurities

Most of the lead fittings are made of a relatively pure metal, however the corrosion of lead will be affected by the presence of impurities such as silver and copper. A sample of lead sheathing (SI 457) from the *Sirius* had a significant amount of an unidentified green lead–copper chloride corrosion product, even though there was only 0.03% copper and 0.01% silver as impurities. Copper corrosion products in the form of $CuSO_4.5H_2O$ and $CuCl_2.2H_2O$ have been found on lead with 0.068% copper impurities on an ancient Roman archaeological site. It has been noted that the presence of metallic and non-metallic inclusions tends to cause accelerated corrosion.[21] The *Zuytdorp* lead ingot (ZT 4179) had a lead content of 99.7% yet had 8.1% of pseudobobolete $Pb_3Cu_4Cl_{10}(OH)_8.2H_2O$ on the surface along with some xanthoconite Ag_3AsS_3. The latter may well be an original sulphide impurity from the smelting of the lead ore and could provide an insight into the source of the lead minerals used in the manufacture of the ingots in 1702. It has been reported that silver diminishes the corrosion of lead, while arsenic tends to promote corrosion in acidic conditions.[22]

Conclusion

The corrosion of lead artefacts on shipwreck sites involves a series of complex hydrolysis and precipitation reactions that leads to a wide variety of minerals being found in the patinas. The nature of the anion precipitated in the patina is seen to provide a sensitive measure of the overall energy state or amount of water movement. Oxide-containing corrosion products are associated with very high energy levels, while sulphate and carbonate dominate the lower-energy zones associated with deeper parts and sheltered gullies of the wreck sites. These data can be utilised by conservators and archaeologists to provide a reference for assessing the forces of deterioration that control the degradation of materials which are subject to corrosion and erosion phenomena. Electrochemical modelling of the early stages of corrosion has given an insight into the way in which the minerals provide protection. On-site measurements on corroding lead confirm that the complex mixture of lead corrosion products is responsible for the low long-term corrosion rates that characterise

marine lead artefacts. The amount of chloride present on the surface of corroded artefacts has been shown to be sensitive to the severity of water movement.

Acknowledgments

We would like to thank Jeffery Beng and Michael Hart for their assistance with SEM and XRD analyses. Richard Garcia prepared the metal coupons and machined them to the correct size. The support of the Norfolk Island Government is gratefully acknowledged for facilitating work on the HMS *Sirius* site. Helpful comments on the manuscript by Luc Robbiola were greatly appreciated.

References

1 I D MacLeod and R. Wozniak, 'Corrosion and Conservation of Tin and Pewter from Sea Water', in *Conservation and Metals/Conservation des Metaux* (London, James and James, 1996).

2 R M Organ, 'The Current Status of the Treatment of Corroded Metal Artefacts', in *Corrosion and Metal Artefacts – a Dialogue between Conservators and Archaeologist and Corrosion Scientists*, ed B F Brown, H C Burnett, W T Chase, M Goodway, J Kruger and M. Pourbaix, NBS Special Publication no 479 (Washington, DC, 1977), 107–142.

3 H S Campbell and D J Mills, 'A Marine Treasure Trove – Metallurgical Investigation', *The Metallurgist and Material Technologist* (October 1977) 551–557

4 P D Moynehan, 'The Corrosion of Metals by Vapours from Air-drying Paints', *Corrosion Science* 5 (1965) 803–814

5 S G Clark and L E Longhurst, 'The Corrosion of Metals by Acid Vapours from Wood', *Journal of Applied Chemistry* 11 (1961) 435–443

6 V Weierter and J Tate, 'The Corrosion of "Lead" Communion Tokens', *Conservation Science in the UK*, ed N Tennent (London, James and James, 1994), 57–59

7 N Tennent, J Tate and L Cannon, 'The Corrosion of Lead Artefacts in Wooden Storage Cabinets' *SSCR Journal* 4, no 1 (1993) 8–11

8 B Gottlieb, C Gottlieb, A Stogren and I Jakobsen, 'A New Method for Cleaning and Conservation of Lead Objects using Hydrogen and Oxygen Plasma', (Paper delivered at the Tenth Triennal Meeting of the International Council of Museums Committee for Conservation, Washington, DC August 1993) 767–771

9 R J Taylor and I D MacLeod, 'Corrosion of Bronzes on Shipwrecks: A Comparison of Corrosion Rates Deduced from Shipwreck Material and from Electrochemical Methods', *Corrosion* 41 (1985): 100–104

10 I D MacLeod, 'Conservation of Corroded Metals – a Study of Ships' Fastenings from the Wreck of HMS *Sirius*', *Ancient and Historic Metals Conservation and Scientific Research*, ed D.A. Scott, J Podany and B B Considine, (Malibu, CA Getty Conservation Institute, 1994), 265–278

11 A M Beccaria, E D. Mor, G Bruno and G Poggi, 'Corrosion of Lead in Sea Water', *British Corrosion Journal* 17 (1982): 87–91

12 D R. Turner and M Whitfield, 'The Reversible Electrodeposition of Trace Metal Ions from Multi-ligand Systems Part II Calculations on the Electrochemical Availability of Lead at Trace Levels in Seawater', *Journal of Electroanalytical Chemistry* 103 (1979): 61–79.

13 G C Tranter, 'Patination of Lead – an Infrared Study' *British Corrosion Journal* 11 (1976): 222–224.

14 W F Linke and A Serdell, *Solubilities of inorganic and metal organic compounds*, Vol. II (Washington: The American Chemical Society 1965), 1275–1313

15 G Milazzo and S Caroli, *Tables of Standard Electrode Potentials* (New York: John Wiley & Sons, 1978), 165–167

16 T F Sharpe, in *Encyclopedia of Electrochemistry of the Elements*, Vol I, ed A J. Bard, (New York Marcel Dekker, 1973), 235–347

17 G Cresswell, 'The Oceanography of the Norfolk Island Vicinity 1988 Expedition Report on the Wreck of HMS *Sirius* (1790)', (Norfolk Island Government Project, Unpublished report compiled by Graeme Henderson, 1989), 46–70

18 M Stanbury, *HMS Sirius 1790. An Illustrated Catalogue of Artefacts Recovered from the Wreck Site at Norfolk Island*, Special Publication No 7 (Fremantle Australian Institute for Maritime Archaeology, 1994), 2–3

19 R G Barradas, K Belinko and E Ghibaudi, 'Effect of Dissolved Gases on the $Pb/PbCl_2$ Electrode in Aqueous Chloride Electrolytes', in *Chemistry and Physics of Aqueous Gas Solutions*, ed. W.A. Adams (Princeton, NJ. Electrothermics and Metallurgy and Industrial Electrolytic Divisions, Electrochemical Society, 1975), 357–372

20 M McCarthy, Personal communication (18 September 1992).

21 P Mattias, G. Maura and G Rinaldi, 'The Degradation of Lead antiquities from Italy', *Studies in Conservation* 29 (1984): 87–92.

22 D Pavlov and T. Rogachev, 'Mechanism of the Action of Silver and Arsenic on The Anodic Corrosion of Lead and Oxygen Evolution at the $Pb/PbO_{(2-x)}/H_2O/O_2/H_2SO_4$ Electrode System', *Electrochimica Acta* 31 (1986) 241–249